

New Particle-In-Cell algorithm for the study of high-amplitude Bernstein-Greene-Kruskal modes in magnetized electron plasmas

F. Peinetti¹, F. Peano¹, G. Coppa¹, and J. Wurtele²

¹ *Dipartimento di Energetica, Politecnico di Torino, Torino, Italy*

² *Department of Physics, UC Berkeley and Center for Beam Physics, LBNL, Berkeley, USA*

Abstract. A numerical technique, developed for the study of the control and excitation of BGK modes in nonneutral plasmas, is presented here. The plasma is highly magnetized and has a large separation of temporal scales. Moreover, while the radial motion of electrons is negligible, the radial boundary conditions change the longitudinal component of the electric field and an accurate calculation requires that electric field include the radial coordinate. To this purpose, a proper decomposition of the system into radial bins allows for an efficient inclusion of its important two-dimensional features. A novel particle loading technique is also presented, which allows for a significant reduction of numerical noise in the initial stage of the excitation, crucial for the subsequent dynamics.

1. INTRODUCTION

Recent experiments [1] have shown the possibility of inducing large-amplitude density oscillations in a pure electron plasma confined in a Penning trap by means of a weak, oscillating external drive of adiabatically-decreasing frequency. In the experiments, density fluctuations slowly emerge from the background and reach amplitudes up to the order of the nominal plasma density, presenting clear evidence for the presence, inside the plasma, of a well-localized moving structure.

The numerical investigation of the phenomenon proves challenging: in fact, the observed nonlinear structures are induced by small-amplitude oscillations of an external perturbing potential and evolve on a time scale much slower than the characteristic time scale of the thermal electron motion inside the trap. As the interesting kinetic features of the phenomenon are essentially one-dimensional (1D), the numerical analysis of these slowly-emerging nonlinear structures does not require the employment of fully two-dimensional (2D) simulations, even though 2D effects need be included in order to perform realistic simulations of the experiments. For these reasons, an ad hoc Particle-In-Cell (PIC) method has been developed, which helped provide deeper physical insights into the dynamics of formation and growth of such structures at a limited computational cost [2].

2. RADIAL DECOMPOSITION ALGORITHM

A Penning trap is composed of a sequence of hollow cylindrical gates, biased at different potentials. The axial confinement of the pure electron plasma is provided by an electrostatic potential well, created after the injection of the plasma, by grounding the central electrodes and properly biasing the end electrodes at a negative potential. The radial confinement of the plasma is provided by a uniform, axial magnetic field B . In [1], one of the electrodes is biased at a weak, oscillating potential. By neglecting the dynamics induced by the slow, $E \times B$ rigid rotation of the whole plasma column, the kinetic equations governing the evolution of the system can be written as

$$\left\{ \begin{array}{l} \frac{\partial f}{\partial t} + v_z \frac{\partial f}{\partial z} + \frac{e}{m_e} \frac{\partial \Phi}{\partial z} \frac{\partial f}{\partial v_z} = 0 \\ \Phi = \varphi + \sum_j \phi^{(j)} \\ \nabla^2 \varphi = \frac{e}{\varepsilon_0} \int f dv_z \\ f(r, z, v_z, t = 0) = \left(\frac{m_e}{2\pi k T_e} \right)^{1/2} g(r) \exp \left[-\frac{m_e v_z^2 / 2 - e\Phi(r, z, t = 0)}{k T_e} \right] \end{array} \right. \quad (1)$$

where f is the electron distribution function (initially assumed Maxwellian in v_z at all radii) and $g(r)$ is the radial profile of the plasma in the initial conditions ($g(r)$ can be assumed constant in time, as any fluid instability comes into play on a much slower time scale). In Eqs. (1), φ is the self-potential and $\phi^{(j)}$ is the potential generated by the j th electrode (the perturbing potential driving the plasma is included here). By considering the following radial decomposition for the distribution function,

$$f(r, z, v_z, t) \simeq \sum_{k=1}^{N_R} f_k(z, v_z, t) S_k(r) \quad (2)$$

where S_k is a double-step function identifying the k th radial bin (centered around the radius r_k and of width Δr_k , see [2] for details), the 2D Vlasov equation can be decomposed into a set of N_R , coupled 1D Vlasov equations for the quantities $\{f_k\}$ of Eq. (2) (being N_R the considered number of radial bins):

$$\frac{\partial f_n}{\partial t} + v_z \frac{\partial f_n}{\partial z} + \frac{e}{m_e} \frac{\partial \bar{\Phi}_n}{\partial z} \frac{\partial f_n}{\partial v_z} = 0 \quad n = 1, \dots, N_R, \quad (3)$$

where $\bar{\Phi}_n(z, t)$ is the average of the total potential over the n th radial bin,

$$\bar{\Phi}_n(z, t) = \frac{1}{r_n \Delta r_n} \int_{\Delta r_n} \Phi(r, z, t) r dr = \bar{\varphi}_n(z, t) + \sum_j \bar{\phi}_n^{(j)}(z, t). \quad (4)$$

The 1D Vlasov equations (4) are linked through the 2D Poisson equation: however, if a Bessel expansion is considered for φ in Poisson equation, the dynamics of the system can be described through a set of coupled 1D equations and can be studied with a set of standard, 1D PIC algorithms. As also discussed in [3] in a more general case, as no radial differential operators are involved in the equations, few radial bins are expected to provide an excellent approximation of the problem and the algorithm is expected to converge for modest values of N_R . This has been verified in the simulations, as can be observed from Figs. 1a-b, which show that the results obtained with the algorithm described here quickly converge to N_R -independent solutions for $N_R \approx 5$.

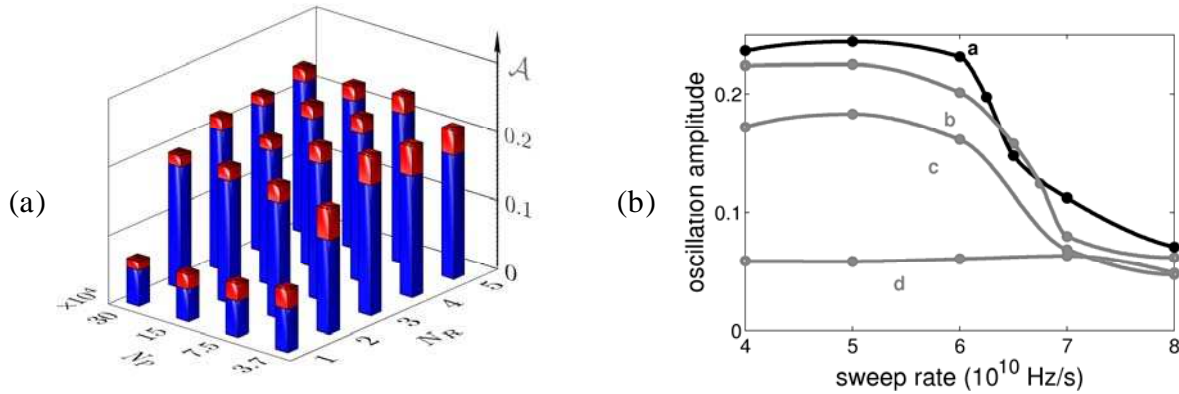


FIG. 1: Response of the system to a frequency chirp from 3.5 to 2 MHz, with a drive amplitude of 0.4 V. In (a), the sweep rate is $5 \cdot 10^{10}$ Hz/s and the final amplitude of the density oscillations has been obtained for different values of N_R and number of computational particles (N_p). The upper parts of the bars indicate the amplitude of the fluctuations for the quantity measured in the simulations). In (b), the response of the system has been calculated for different sweep rates: the reference results of curve a ($N_R=5$, $N_p=3 \cdot 10^5$) are well reproduced with only $N_p=6 \cdot 10^4$, if the number of radial bins is preserved (curve b). The threshold observed in the sweep rate, around $7 \cdot 10^{10}$ Hz/s, is recovered even with $N_R=2$ (curve c) but is lost in the single-bin approximation (curve d).

3. ERGODIC LOADING

The classic loading algorithm employed in many PIC simulations (often referred to as *quiet start*) is not convenient in the present case, in which the behavior of an electron distribution deeply-trapped in an external potential well has to be investigated. In fact, the axial bounce of particles can lead to numerical problems responsible for unphysical density fluctuations and high numerical noise (see Fig.2a). The problem has been solved by developing a novel loading procedure, called ergodic loading. Instead of being initially positioned on cold, parallel beams, the particles are now positioned on the closed trajectories of test particles in the equilibrium total potential, equally spaced in phase within the bounce period and properly

weighed, in order to reproduce the correct energy distribution associated with the Maxwellian equilibrium [2]. The improvement in terms of noise suppression is relevant, especially in the early phase of the simulations (see Fig. 3), and for this reason we think this numerical procedure can be useful also in other situations of interest for PIC simulations.

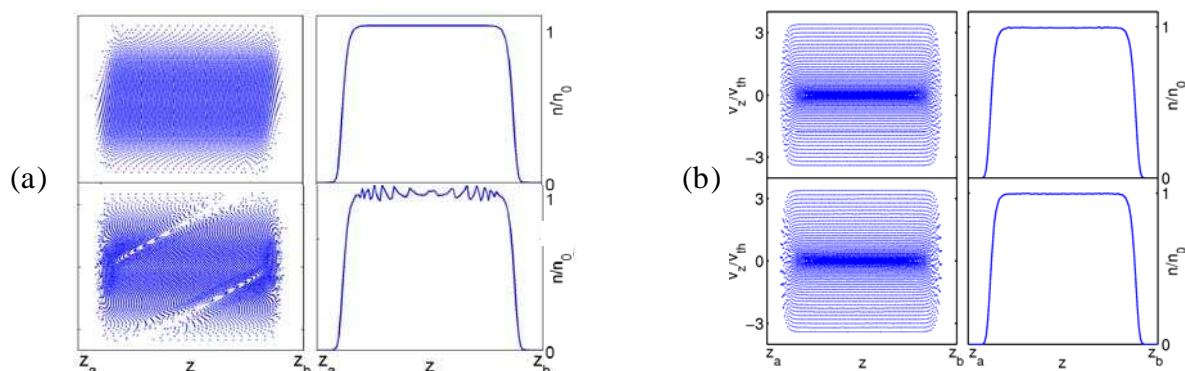


FIG. 2: (a) evolution of the equilibrium, initial plasma distribution in phase-space (left column) and of the corresponding axial density profile (right column), in the case of standard quiet start: the upper graphs refer to the initial distribution, while the lower graphs refer to a time of the order of the thermal bounce period. The phase-space pattern responsible for density fluctuations are clearly visible. (b) same of (a), but with the ergodic loading of particles.

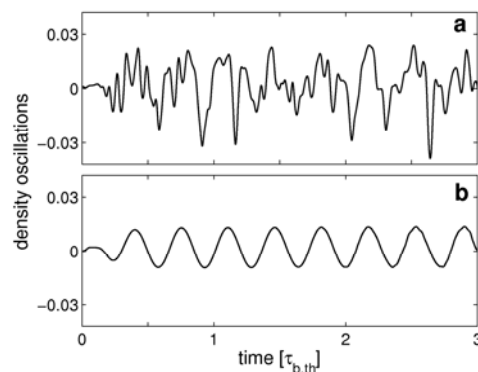


FIG. 3: Time evolution of the density oscillations, as observed on one end of the plasma column, during the early phase of the excitation process. In (a), $3.6 \cdot 10^5$ particles have been loaded according to the classic quiet start procedure, while, in (b), 10^5 particles have been loaded according to the ergodic loading procedure proposed here.

REFERENCES

- [1] W. Bertsche *et al.*, Phys. Rev. Lett. 91, 265003 (2003).
- [2] F. Peinetti *et al.*, J. Comput. Phys. 2006, in press.
- [3] G. Manfredi *et al.*, JCP 121, 298 (2005)